Materials Research. 2019; 22(5): e20190014
DOI: http://dx.doi.org/10.1590/1980-5373-MR-2019-0014

Corrosion Resistance of TiO_2-ZrO_2 Nanocomposite Thin Films Spin Coated on AISI 304 Stainless Steel in 3.5 wt. % NaCl Solution

***Mohammad Younes Al-Daraghmeh*[a], *Mohammed Taiseer Hayajneh*[a]*, *Mohammed Ali Almomani*[a]**

[a]*Industrial Engineering Department, Faculty of Engineering, Jordan University of Science and Technology, P.O. Box030, Irbid,2110, Jordan*

Received: January 9, 2019; Revised: July 19, 2019; Accepted: October 2, 2019

Utilizing high chromium and nickel content in AISI 304 steel confers its good corrosion resistance. However, the high content of chromium and nickel increases the steel susceptibility to corrosion caused by the high concentration of chlorine. Consequently, the electrochemical and mechanical performance of the steel degrades. In this study, the effect of adding a layer containing a gelatin-dispersed mix of TiO_2-ZrO_2 nanoparticles on the corrosion rate and critical pitting potential of AISI 304 steel is studied. Two mix ratios of TiO_2-ZrO_2 nanoparticles to gelatin (0.5:0.5, 0.3:0.7) were used. Three different fractions of nanoparticles (1 wt. %, 2 wt. %, 3 wt. %) were used for each ratio. Potentiodynamic polarization examinations were used to measure the corrosion rate and the critical-pitting potential of the spin-coated AISI 304 steel in a simulated environment containing 3.5 wt. % NaCl. Scanning electron microscopy (SEM) and energy dispersive x-ray (EDX) were used to study the morphology of the coated surfaces and the elemental composition of the nanocomposite coatings. The results show that the hybrid TiO_2-ZrO_2 nanoparticles coatings significantly improved the uniform and localized corrosion of the AISI 304 steel. Moreover, the results confirm the formation of homogeneous, stable, and crack-free coatings.

Keywords: *Titanium dioxide, Zirconium dioxide, gelatin, corrosion resistance, AISI 304 stainless steel, nanocomposites coatings.*

1. Introduction

The AISI 304 steel is utilized in a wide variety of industrial and household applications in addition to food processing equipment because of its high mechanical and corrosion resistance conferred by its content of chromium and nickel[1-4]. However, it is susceptible to pitting in environments containing a high concentration of chlorine[5]. The problem is addressed using several techniques including grain strengthening[6-8], surface treatment with alloying elements[9], or surface coating by protecting layers[10-11]. The first two techniques are expensive and take a long time while the third technique is easy to perform.

Titanium dioxide (TiO_2) and Zirconium dioxide (ZrO_2) are among the most commonly used ceramic particles oxides as corrosion resistance coatings[12-16]. The use of coatings with a single oxide exhibits some issues owing to the presence of pores and cracks in the coatings[17].

Hybrid or multi oxides coatings can potentially combine the properties of all its constituent components. Also, the properties of these coatings can be tailored by controlling the concentrations of its constituents such as the mix ratio of nanoparticles to overcome the limitations of coating with a single oxide. Hybrid coatings of TiO_2-ZrO_2 over different kinds of steel substrates were studied using several methods to improve the corrosion resistance of the underlying substrates. Bu et al.[18] studied the behaviour of nanostructured TiO_2-ZrO_2 layers on AISI-202 stainless steel created by the sol-gel dip-coating method in a 5 wt. % NaCl solution at room temperature. Based on this study, the coating enhances the corrosion protection of AISI-202 stainless steel. Abd El-Lateef and Khalaf[19] investigated the corrosion behaviour of nanocomposite multi TiO_2-ZrO_2 layers on carbon steel created by the sol-gel dip-coating technique in 0.1M HCL solution at 50°C. The electrochemical analysis results showed that there is an improvement in carbon steel corrosion resistance. Cai et al.[20] used a hybrid TiO_2-ZrO_2 coating on AISI 304 steel by the liquid-phase deposition method. The corrosion resistance of steel was evaluated in simulated geothermal water at 50°C by a potentiodynamic polarization test. The results reveal that the hybrid TiO_2-ZrO_2 coating significantly enhances the AISI 304 steel corrosion resistance.

Gelatin is one of the promising coating materials for metallic implants because of its bio-compatibility, good adhesion characteristics, and its acceptable cost. Recently, researchers used gelatin as matrix materials in ceramic bio composites in which ceramic nanoparticles are dispersed[21-23].

This research investigates the corrosion behaviour of the spin-coated AISI 304 steel by adding a layer having a mix of TiO_2-ZrO_2 nanoparticles dispersed in gelatin in a simulated marine environment containing chloride ion. The protection against corrosion of selected hybrid TiO_2-ZrO_2 nanoparticles at different weight percentages and mix ratios dispersed in a gelatin matrix and created by the spin-coating process is investigated in a 3.5 wt. % NaCl solution.

*e-mail: hayajneh@just.edu.jo

2. Experimental Procedure

2.1 Substrates and their Preparation

Specimens of AISI 304 steel with area and thickness of 55 $mm^2$and 1 mm, respectively, were used as substrates. Before coating, several steps were followed to treat the substrates to clean them from dirt and contaminations. They were chemically etched to improve coating-substrate adhesion. First, the specimens were etched by a solution of nitric HNO_3 (70%) and H_2O_2 (30%). Second, the specimens were sonicated in acetone and deionized water respectively for 15 minutes for each step. Third, a hot air stream was used to dry the substrates.

2.2 Preparation of gelatin-hybrid TiO_2-ZrO_2 coatings

Several nanocomposites coatings containing a mixture of two types of ceramic nanoparticles dispersed in polymer mixture were developed. The used ceramic nanoparticles were obtained from the US Research Nanomaterials company, U.S.A. The purity, size, and density of the used nanoparticles are provided in Table 1. Gelatin type A porcine skin with molecular weight of 50,000-100,000 (Sigma) was used as a matrix material to hold the ceramic nanoparticles in the developed nanocomposites coatings. The procedure described by Torkaman et al.[23] was followed to prepare the gelatin matrix.

Table 1. Purity, size, and density of the used nanoparticles.

Nanoparticles	Purity (%)	Size (nm)	Density (g/cm^3)
TiO_2	≥99	10-25	3.90
ZrO_2	≥99	40	5.89

Two main types of nanocomposites coatings were developed: the first type with a mix ratio of TiO_2:ZrO_2 set to 0.5:0.5 and denoted composite coating A, the second type with a mix ratio of TiO_2:ZrO_2 set to 0.3:0.7 and denoted composite coating B. For each type of the composite coatings, three weight fractions of the hybrid nanoparticles (1, 2, 3) wt. % were used. The nanocomposites coatings were prepared at room temperature. After complete gelatin dissolution and adding the appropriate percentages of the nanoparticles, a magnet stirrer (Dragon Lab, MS-H-S) was used for 24 hours at room temperature to ensure homogeneous dispersion of nanoparticles in the suspension. Cross-linking is essential to stabilize the gelatin structure in water. Ethyl-3-(3-dimethylaminopropyl) carbodiimide (EDC, Sigma) was used as a cross-linking agent. Nine wt. % EDC solutions in ethanol were added to the suspension and magnetically stirred for 6 hours at 50°C.

A precision spin-coater (KW-4A, Chemat Technology Inc.) equipped with a vacuum pump (Gast Manufacturing) was utilized to coat the AISI 304 steel substrates with the developed hybrid gelatin nanocomposite coatings. Spinning speeds of 250 rpm (low) and 2500 rpm (high) were chosen for all coated samples while spinning time was chosen for all coated samples to be 15 seconds for the low coating speed and 30 seconds for the high coating speed.

2.3 Characterization of the nanocomposite coatings

The surface morphology of the coated substrates was investigated by scanning electron microscopy (SEM) with energy dispersive X-ray analysis (EDX) before the corrosion test to investigate the homogeneity and dispersion of the nanoparticles within the gelatin matrix, and after the corrosion test to investigate the effect of corrosion test on the morphology of the coated samples. EDX was used for elemental analysis and chemical characterization of the surfaces of substrates and corrosion test products. The phase identification of the coated samples was performed using X-ray diffraction (XRD) to confirm the presence of hybrid TiO_2-ZrO_2 nanoparticles within the coating on the AISI 304 steel substrates. Direct current polarization (DCP) test was used to examine corrosion behaviour of the coated AISI 304 steel substrates. Gamry potentiostat Ref 600 corrosion testing module was used with graphite as a counter while a saturated calomel electrode (SCE) was used as a reference.

2.4 Statistical analysis

The statistical significance of the examined coating type of samples was measured using a one-way ANOVA analysis by Minitab software (Version 18). Differences were chosen to be significant for P-value < 0.05.

3. Results and Discussion

3.1 Chemical characterization of hybrid TiO_2-ZrO_2 nanocomposite coatings

Figure 1a shows the uncoated AISI 304 steel surface before conducting the corrosion test. It can be seen that the surface has a tube-shaped form that was created during the polishing process by detaching some material from the surface. Many scratch lines also can be seen in parallel with the polishing lines**.** Figure 1b shows the SEM images of a pure gelatin-coated sample before the corrosion test. It can be seen that the surface is totally covered by a smooth, homogeneous, and well-distributed gelatin layers without cracks or defects. Figure 1c shows the SEM images of hybrid TiO_2-ZrO_2 coating with a mix ratio of 0.5:0.5 containing 2 wt. % nanoparticles before the corrosion test. It is shown that the coating layer covered the entire AISI 304 steel surface while the hybrid TiO_2-ZrO_2 coatings distributed uniformly throughout the gelatin. Also, the difference is shown between ZrO_2 and TiO_2 nanoparticles sizes; ZrO_2 has a larger average size as compared to TiO_2 nanoparticles, which affects the coating nanoscale roughness. The SEM images show the nano size of hybrid TiO_2-ZrO_2 (0.5:0.5) nanoparticles in the gelatin coating in addition to some micro size agglomerations of ZrO_2 nanoparticles. Figure 1d shows a hybrid TiO_2-ZrO_2 coating with a mix ratio of 0.3:0.7 containing 2 wt. % nanoparticles before the corrosion test. As shown, the coating layer covered the entire AISI 304 steel surface and the hybrid TiO_2-ZrO_2 0.3:0.7 wt. nanoparticles, which are distributed uniformly throughout the gelatin.

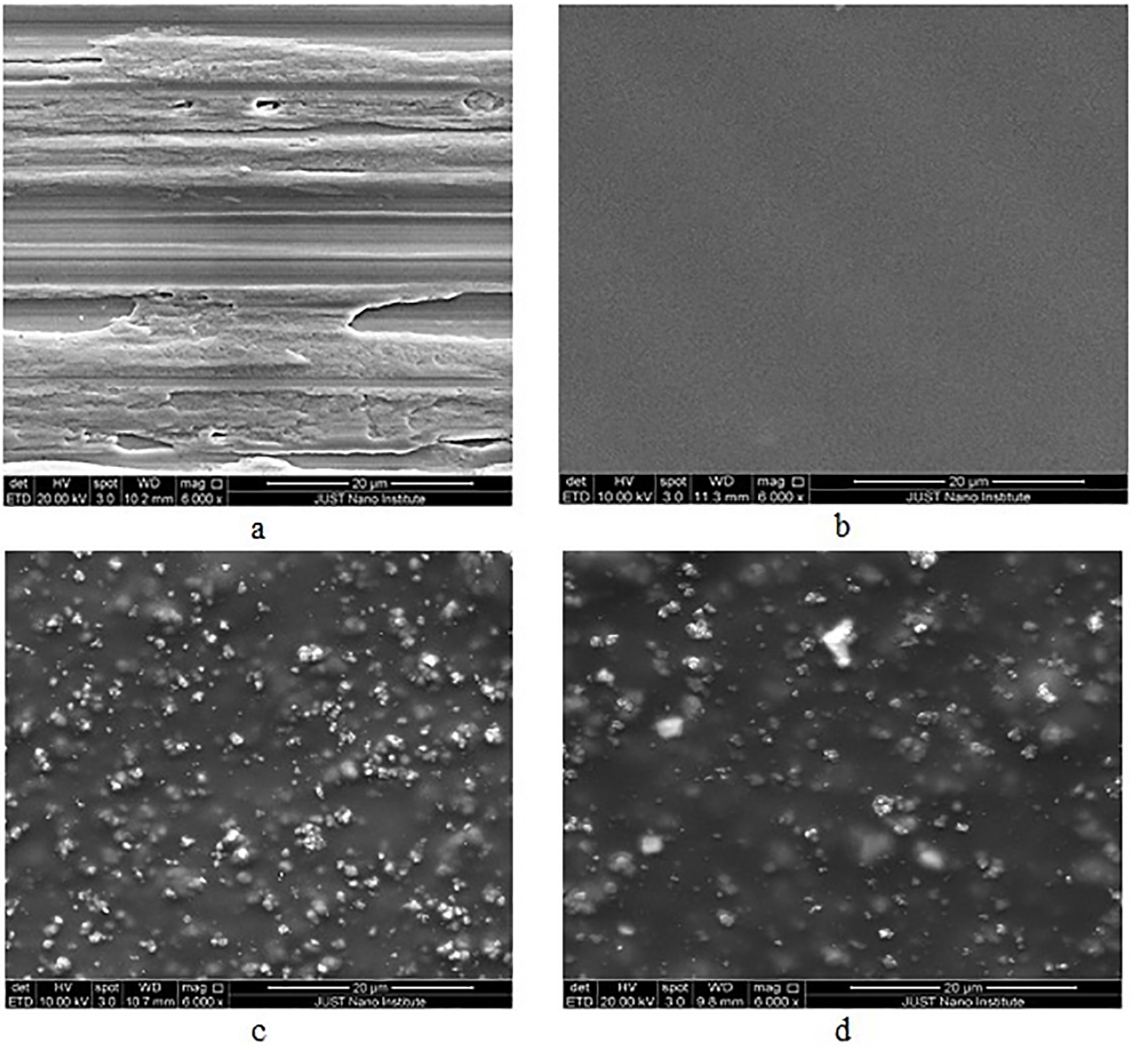

Figure 1. (a) Surface morphology of the AISI 304 steel before conducting the corrosion test, (b) SEM image of pure gelatin-coated sample before the corrosion test, (c) SEM image of hybrid TiO_2-ZrO_2 coating with mix ratio 0.5:0.5 containing 2 wt. % nanoparticles before the corrosion test, (d) SEM image of hybrid TiO_2-ZrO_2 coating with mix ratio 0.3:0.7 containing 2 wt. % nanoparticles before the corrosion test.

Figures 2a and 2b show the EDX spectrum and the quantitative analysis of the coated AISI 304 steel with hybrid TiO_2-ZrO_2 coating with mix ratios of 0.5:0.5 and 0.3:0.7 containing 2 wt. % nanoparticles before the corrosion test, respectively. Both the EDX spectrum and the quantitative analysis prove the presence of hybrid TiO_2-ZrO_2 nanoparticles in the gelatin coating before conducting the corrosion test.

Figure 3 shows the uncoated AISI 304 steel surface morphology after the corrosion testing. A brittle salt layer with many cracks filled with the corrosion products covered the whole surface. The cracks formation is attributed to the internal stresses caused by the released gases during the cathodic reactions, or it can be formed as a result of the salt layer. Also as seen in the Figure, the uncoated AISI 304 steel surface filled with many pits of different sizes. The gelatin coating layer without nanoparticles completely deteriorated and failed to protect the AISI 304 steel surface from corrosion as shown in Figure 4. The dispersion of hybrid TiO_2-ZrO_2 of 0.5:0.5 mix ratio enhances the performance of the gelatin coating in protecting the AISI 304 steel as proved by the corrosion test, which does not reveal any obvious cracks or pits while the ZrO_2 nanoparticles appear clearly on the surface as shown in Figure 5. As well, the coating is still stable after conducting the corrosion test with only shallow cracks caused by the salt layer; ZrO_2 nanoparticles appear clearly on the surface. Generally, the hybrid TiO_2-ZrO_2 (0.3:0.7) coating shows a better surface morphology and cracks propagation resistance after the corrosion test than the hybrid TiO_2-ZrO_2 0.5:0.5 nanoparticles coating as shown in Figure 6. Therefore, it is a reasonable indicator of the stability and the functionality of this coating. Figures 7a and 7b represent the EDX spectrum and quantitative analysis of the coated AISI 304 steel with hybrid TiO_2-ZrO_2 0.5:0.5 and 0.3:0.7 nanoparticles dispersed in the gelatin after the corrosion test, respectively. Figure 7 proves the presence of TiO_2 and ZrO_2 nanoparticles in the gelatin coating after conducting the corrosion test.

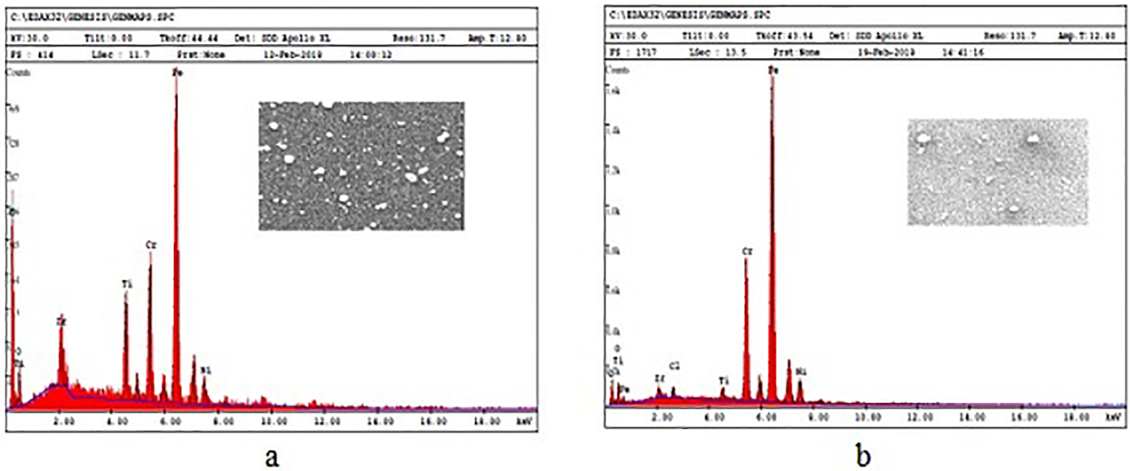

Figure 2. (a) EDX spectrum and quantitative analysis of the coated AISI 304 steel with hybrid TiO_2-ZrO_2 coating with a mix ratio of 0.5:0.5 containing 2 wt. % nanoparticles before the corrosion test, (b) EDX spectrum and quantitative analysis of the coated AISI 304 steel with hybrid TiO_2-ZrO_2 coating with a mix ratio of 0.3:0.7 containing 2 wt. % nanoparticles before the corrosion test.

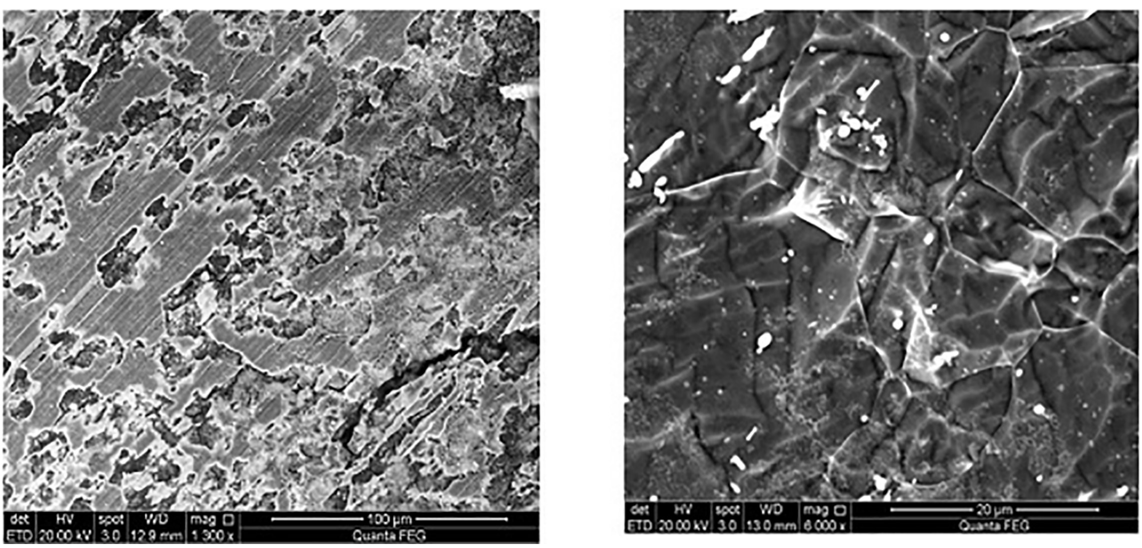

Figure 3. Surface morphology of the uncoated AISI 304 steel after conducting the corrosion test.

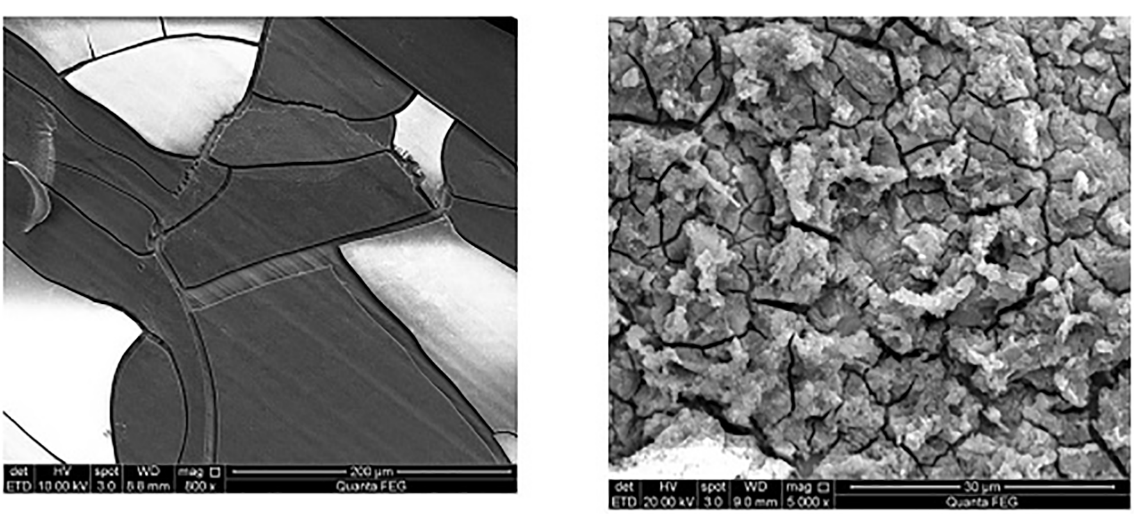

Figure 4. Surface morphology of the coated AISI 304 steel with gelatin after conducting the corrosion test.

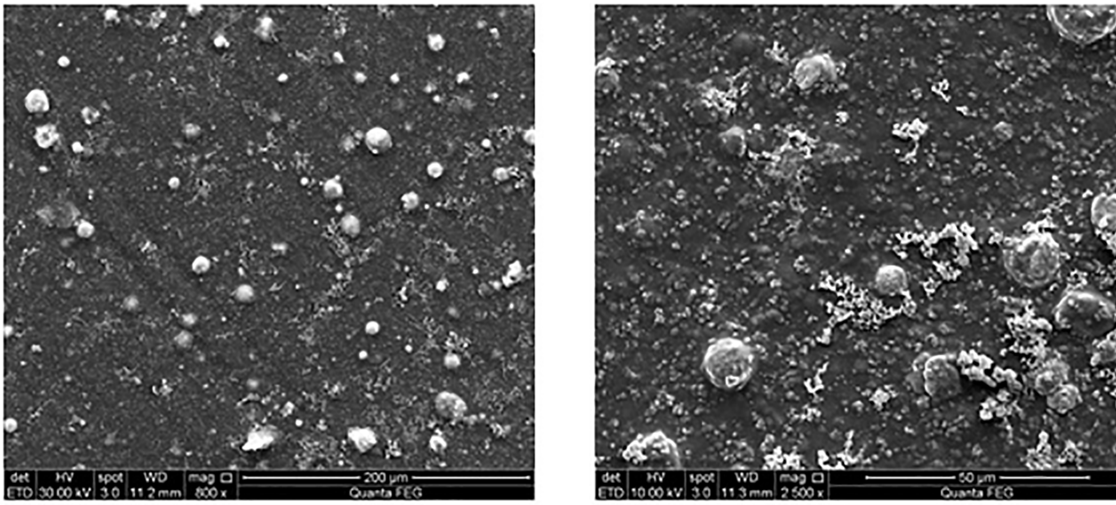

Figure 5. SEM images of the hybrid TiO_2-ZrO_2 coating with a mix ratio of 0.5:0.5 containing 2 wt. % nanoparticles after the corrosion test.

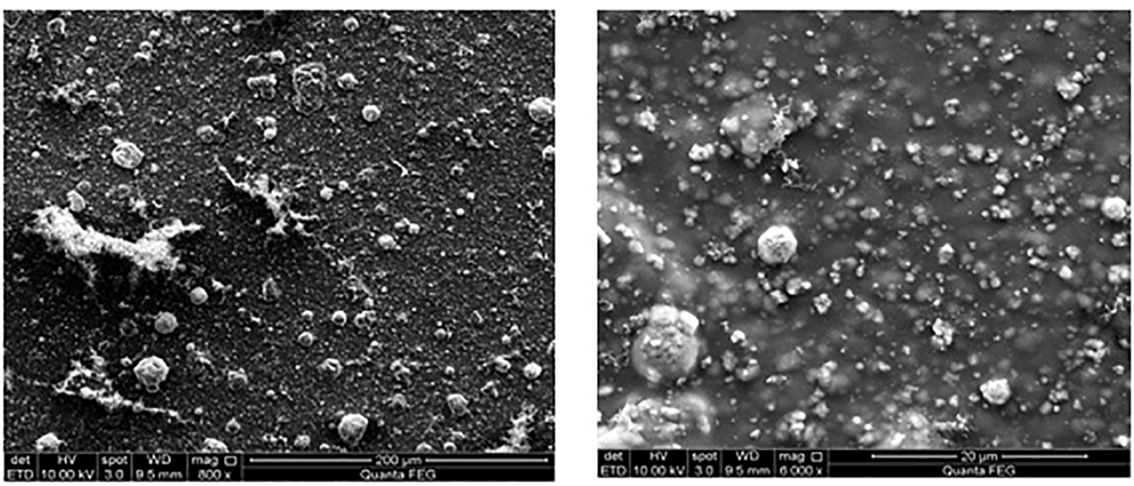

Figure 6: SEM images of the hybrid TiO_2-ZrO_2 coating with a mix ratio of 0.3:0.7 containing 2 wt. % nanoparticles after the corrosion test.

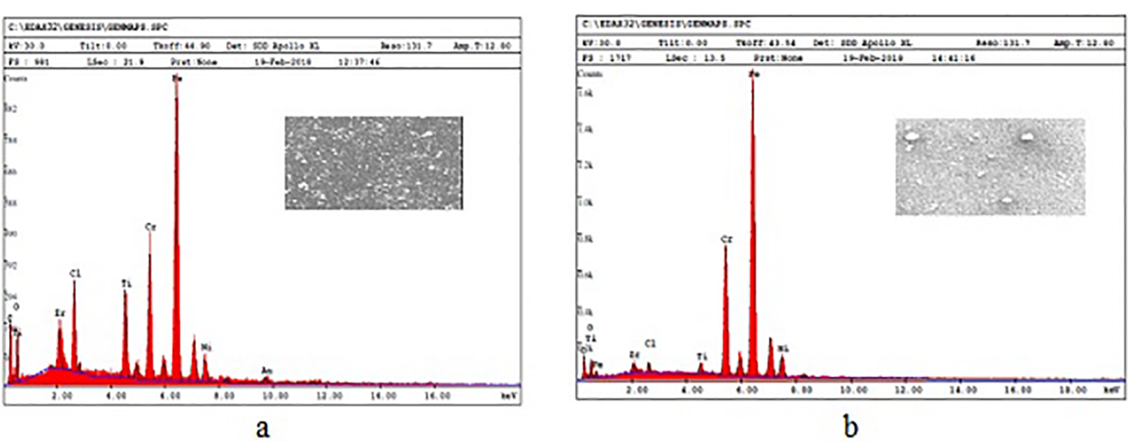

Figure 7: (a) EDX spectrum and quantitative analysis of the coated AISI 304 steel with hybrid TiO_2-ZrO_2 coating with a mix ratio of 0.5:0.5 containing 2 wt. % nanoparticles after the corrosion test, (b) EDX spectrum and quantitative analysis of the coated AISI 304 steel with the hybrid TiO_2-ZrO_2 coating with a mix ratio of 0.3:0.7 containing 2 wt. % nanoparticles after corrosion test.

3.2 XRD analysis

X-ray diffraction (XRD) analysis was applied to confirm the presence of TiO_2 and ZrO_2 nanoparticles within the gelatin coating. As shown in Figure 8, the gelatin does not have any clear peak in XRD pattern, which is compatible with its amorphous nature, while the XRD pattern of gelatin-hybrid TiO_2-ZrO_2 of 0.5:0.5 mix ratio comprises the main characteristic peaks of ZrO_2 at 2Theta (blue arrows: 23.929, 24.278, 28.046, 28.461, 31.301, 33.93 and 35.1 degrees), and the main characteristic peaks TiO_2 at 2Theta (green arrows: 24.88, 25.155, 37.71, 38.47, 40.59, 50.02, 65.52 degree) proving the presence of hybrid TiO_2-ZrO_2 nanoparticles in this coating (card no. (01-074-0815))

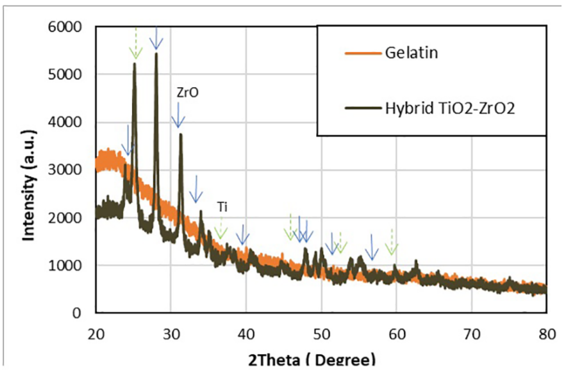

Figure 8. XRD pattern of gelatin and gelatin-TiO_2 –ZrO_2 (0.5:0.5) nanoparticles on a fused-glass substrate.

3.3 Electrochemical corrosion investigation

Table 2 summarizes the corrosion rates, corrosion potentials (E_{corr}), corrosion current densities (I_{corr}), and critical pitting potentials (E_{pit}) that were obtained from the Tafel scans for all examined samples. Chi-squared values were used to give information about the goodness of Tafel fit performed on the samples. The lower Chi-Squared value indicates that the performed fit is good. The fit is considered acceptable if the Chi-squared value is less than 100[24]. Based on Table 2, I_{corr} value can imply significant information about the corrosion behavior since it has a proportional relationship with the corrosion rate. The sample that has the least corrosion current density experiences the best corrosion resistance. In contrast with the $E_{corr,}$ values that cannot give any specific information about the corrosion trend.

Figures 9 and 10 show the potentiodynamic polarization curves of the AISI 304 steel spin coated with hybrid TiO_2-ZrO_2 coating with a mix ratio of 0.5:0.5 and 0.3:0.7 containing different weight percentages of nanoparticles dispersed in gelatin, respectively. It is shown that coating AISI 304 steel with only gelatin does not achieve any improvement in the corrosion resistance. Dispersing hybrid TiO_2-ZrO_2 (mix ratio of 0.5:0.5) nanoparticles in the gelatin reduces the corrosion rate. Such enhancement is attributed to the ceramic protective barrier on the AISI 304 stainless steel surface. The corrosion rate decreases as the fraction of nanoparticles weight increases. Such results can be explained by the poor mixing of nanoparticles and distribution throughout the gelatin matrix, which could increase the macro porosity between the two different nanoparticle average sizes of TiO_2 and ZrO_2, 10-20 nano and 40 nano respectively. But as the nanoparticles wt. % increases, the hybrid nanoparticles distribute more homogeneously through the gelatin and the porosity decreases significantly between the TiO_2 and ZrO_2 nanoparticles. Therefore, the coating becomes more effective in enhancing the corrosion resistance of the AISI 304 steel[25]. Dispersing hybrid nanoparticles TiO_2-ZrO_2 of 0.3:0.7 mix ratio in the gelatin also reduces the corrosion rate. Such enhancement is attributed to the ceramic protective barrier on the AISI 304 stainless steel surface. The results show also that increasing the hybrid nanoparticles wt. % in gelatin to 3 wt. % improves the AISI 304 steel corrosion resistance contrary to 1 and 2 wt. %, whereas the hybrid nanoparticles (at 3 wt. %) distribute more homogeneously with less porosity throughout the gelatin matrix; the coating became more effective in enhancing the corrosion resistance of the AISI 304 steel.

Table 2. Corrosion rates and electrochemical constant values for the uncoated AISI -304 steel sample and the AISI 304 steel coated with hybrid TiO_2-ZrO_2 nanoparticles dispersed in gelatin samples.

The Examined Samples	Percentage (wt. %)	E_{corr} (mV vs. SCE)	I_{corr} (μA/cm²)	Corrosion rate (10^{-3}) mpy	Chi-squared	E_{pit} (V vs. SCE) (mV)
Uncoated AISI 304 steel	-	-67.7	0.126	9.914	3.89	265
Coated AISI steel with gelatin only	-	-87.0	0.154	12.130	3.51	355
TiO_2- ZrO_2 0.5:05	1	-157.0	0.041	3.264	4.32	403
TiO_2- ZrO_2 0.5:05	2	-118.0	0.045	3.507	7.02	367
TiO_2- ZrO_2 0.5:05	3	-169.0	0.046	3.584	4.26	410
TiO_2- ZrO_2 0.3:0.7	1	-155.0	0.048	3.740	3.93	374
TiO_2- ZrO_2 0.3:0.7	2	-164.0	0.053	4.158	3.71	396
TiO_2- ZrO_2 0.3:0.7	3	-54.9	0.033	2.582	30.43	370

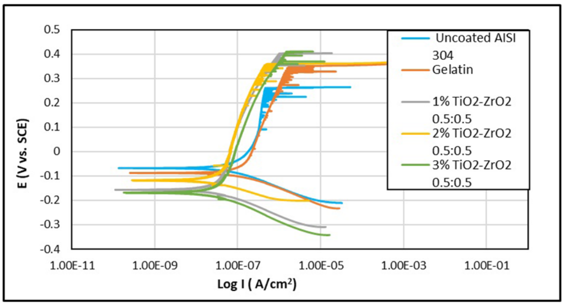

Figure 9. The potentiodynamic polarization curves of the AISI 304 steel coated with hybrid TiO_2-ZrO_2 coating with mix ratio 0.5:0.5 and different weight percentages (1% wt., 2% wt., 3% wt.) of nanoparticles dispersed in gelatin.

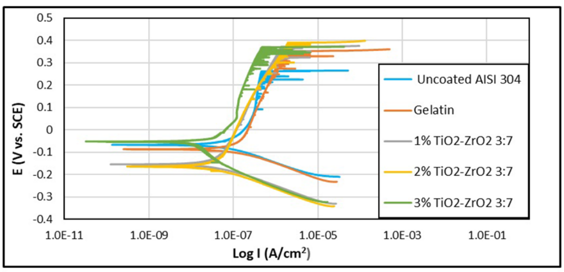

Figure 10. Potentiodynamic polarization curves of the AISI 304 steel coated with hybrid TiO_2-ZrO_2 coating with mix ratio 0.3:0.7 and different weight percentages (1% wt., 2% wt., 3% wt.) of nanoparticles dispersed in gelatin.

Figure 11 shows the corrosion rate of the AISI 304 steel coated with hybrid TiO_2-ZrO_2 coating with mix ratios 0.5:0.5, 0.3:0.7 and different weight percentages (1% wt., 2% wt., 3% wt.) of nanoparticles dispersed in gelatin, as well the corrosion rate of the uncoated AISI 304 steel and the coated AISI 304 steel with gelatin only.

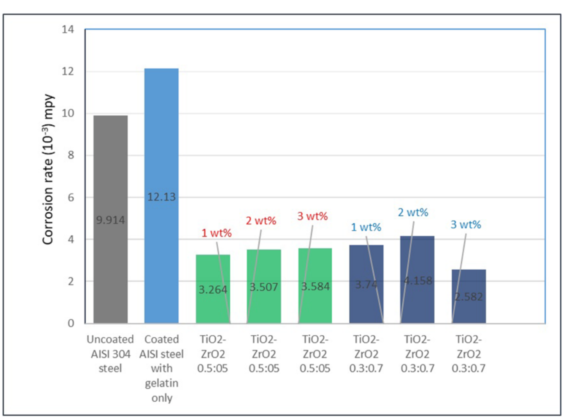

Figure 11. Corrosion rate (10^{-3}mpy) of the AISI 304 steel coated with hybrid TiO_2-ZrO_2 coating with mix ratios 0.5:0.5, 0.3:0.7, and different weight percentages (1% wt., 2% wt., 3% wt.) of nanoparticles dispersed in gelatin, as well the corrosion rate of the uncoated AISI 304 steel and the coated AISI 304 steel with gelatin only.

Figure 12 shows the critical pitting potential behavior of the AISI 304 steel coated with hybrid TiO_2-ZrO_2 coating with mix ratios 0.5:0.5, 0.3:0.7, and different weight percentages (1, 2, 3% wt.) of nanoparticles dispersed in gelatin, as well the critical pitting potential behavior of the uncoated AISI 304 steel and the coated AISI 304 steel with gelatin only. As shown, the hybrid TiO_2-ZrO_2 (0.5:0.5, 0.3:0.7) nanoparticles coatings improve the critical pitting potential of the AISI 304 steel significantly due to the formation of stable

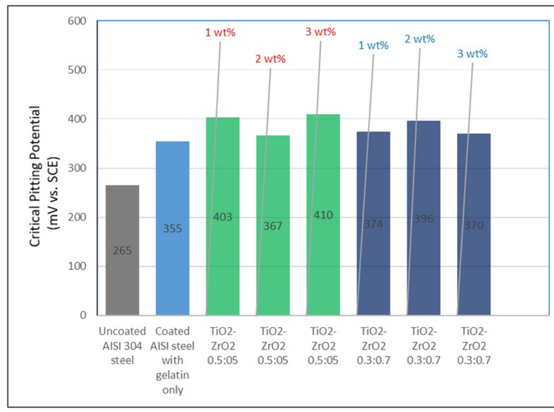

Figure 12: Critical pitting potential behavior of the AISI 304 steel coated with hybrid TiO_2-ZrO_2 coating with mix ratio 0.5:0.5, 0.3:0.7, and different weight percentages (1% wt., 2% wt., 3% wt.) of nanoparticles dispersed in gelatin, as well the critical pitting potential behavior of the uncoated AISI 304 steel and the coated AISI 304 steel with gelatin only.

coating layers on the AISI 304 steel surface compared with the unstable oxide film on the uncoated AISI 304 steel, which could not sufficiently protect against pitting corrosion[23]. The results show that increasing the hybrid nanoparticles weight percentages slightly enhances the critical pitting potential to more positive values, whereas increasing the nanoparticles wt. % causes the hybrid nanoparticles to distribute more homogeneously through the gelatin matrix, while the porosity increases significantly. Therefore, the coating becomes more effective in reducing the pit initiation tendency.

3.4 Statistical analysis

The statistical significance of the coating type was measured using a one-way ANOVA analysis by Minitab software (Version 18). Differences were chosen to be significant for P-value < 0.05. Four groups of specimens were examined: uncoated AISI 304 stainless steel, coated AISI 304 steel with gelatin only, hybrid TiO_2-ZrO_2 0.5:0.5 nanoparticles coating, and hybrid TiO_2-ZrO_2 0.3:0.7 nanoparticles coating. Statistical procedures based on the analysis of variance methods were used to analyse the data. Tables 3 and 4 summarize respectively the factor information and analysis of variance results of the corrosion rates of all tested samples. Figure 13 shows the interval plot of the corrosion rate (10^{-3} mpy) versus the coating type. ANOVA results indicate clearly that there is a statistically significant difference between the corrosion rate of the coating types, uncoated AISI 304 steel, coated AISI 304 steel with gelatin only, hybrid TiO_2-ZrO_2 0.5:0.5 nanoparticles coating, and hybrid TiO_2-ZrO_2 0.3:0.7 nanoparticles coating, whereas the p-value is less than 0.05. Table 5 summarizes the analysis of variance results of the critical pitting potential for all coating types: uncoated AISI 304 steel, coated AISI 304 steel with gelatin only, hybrid TiO_2-ZrO_2 0.5:0.5 nanoparticles coating, and hybrid TiO_2-ZrO_2 0.3:0.7 nanoparticles coating. Also, Figure 14 shows the interval plot of the critical pitting potential versus the coating type. ANOVA results indicate clearly that there is a statistically significant difference between the corrosion rate of the four coating types, uncoated AISI 304 steel, coated AISI 304 steel with gelatin only, hybrid TiO_2-ZrO_2 0.5:0.5 nanoparticles coating, and hybrid TiO_2-ZrO_2 0.3:0.7 nanoparticle coating, whereas the p-value is less than 0.05. It is shown that all coating types can significantly improve the critical pitting potential of the uncoated AISI 304 steel. This characteristic is due to the formation of the coating layers on the AISI 304 stainless steel surface compared with the unstable oxide film on the uncoated AISI 304 stainless steel, which could not sufficiently protect against pitting corrosion[23].

Table 3. Coating type factor levels.

Factor	Levels	Values
Coating Type	4	Uncoated AISI 304 steel; Coated steel with gelatin only; coated steel with TiO_2- ZrO_2 0.5:05; Coated steel with TiO_2- ZrO_2 0.3:0.7

Table 4. ANOVA test results of the corrosion rate versus coating type.

Source	DF	Adj SS	Adj MS	F-Value	P-Value
Coating Type	3	120.6	40.21	3.68	0.032
Error	18	196.7	10.93		
Total	21	317.3			

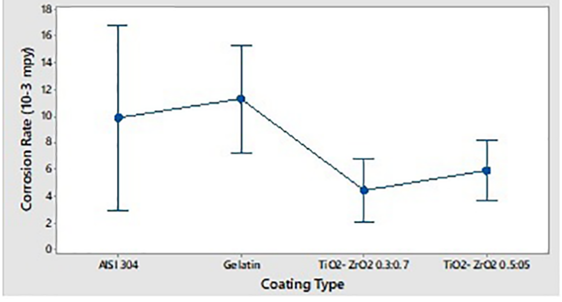

Figure 13. Interval plot of corrosion rate (10^{-3} mpy) versus the coating type.

Table 5. ANOVA test results of the critical pitting potential (E_{pit}) versus coating type.

Source	DF	Adj SS	Adj MS	F-Value	P-Value
Coating Type	3	14704	4901.4	14.46	0.000
Error	18	6102	339.0		
Total	21	20806			

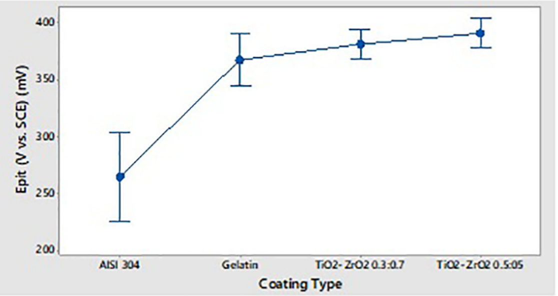

Figure 14: Interval plot of the critical pitting potential (V vs. SCE) (mV) versus the examined sample type.

4. Conclusions

In this study, gelatin-hybrid nanocomposite coatings were created using the spin technology over the AISI 304 steel substrates. The effect of the weight fraction and mix ratio of TiO_2-ZrO_2 nanoparticles dispersed in the gelatin matrix of composites on the corrosion rate and the critical pitting potential of the underlying substrates were studied. Based on the results of this study, we draw the following conclusions:

1. Coating the AISI304 steel with gelatin only does not improve the corrosion rate.
2. Hybrid nanocomposites coatings with a mix ratio of 0.3:0.7 have corrosion resistance that outperforms the resistance of coatings with a mix ratio of 0.5:0.5.
3. Hybrid TiO_2-ZrO_2 nanoparticles dispersed in the gelatin matrix could significantly enhance the AISI 304 steel electrochemical properties compared with the uncoated AISI 304 steel and gelatin-coated samples.
4. The statistical analysis results indicate clearly that there is a significant difference between the corrosion rate of the four coating types (uncoated AISI 304 steel, coated AISI 304 steel with gelatin only, hybrid TiO_2-ZrO_2 0.5:0.5 nanoparticles coating, and hybrid TiO_2-ZrO_2 0.3:0.7 nanoparticles coating). It is shown that all coating types can improve the critical pitting potential of the uncoated AISI 304 steel significantly. This improvement is due to the formation of the coating layers on the AISI 304 stainless steel surface compared with the unstable oxide film on the uncoated AISI 304 stainless steel, which could not sufficiently protect against pitting corrosion.

Acknowledgments

This work was supported by a grant from the Deanship of Scientific Research at Jordan University of Science and Technology (JUST) with grant no. 39/2017. The authors thank JUST engineering workshop staff for their help on this work.

References

1. Dirviyam PS, Palanisamy C. Optimization of surface roughness of AISI 304 steel austenitic stainless steel in dry turning operation using Taguchi design method. *Journal of Engineering Science and Technology*. 2010;5(3):293-301.

2. Martin M, Weber S, Izawa C, Wagner S, Pundt A, Theisen W. Influence of machining-induced martensite on hydrogen-assisted fracture of AISI type 304 steel austenitic stainless steel. *International Journal of Hydrogen Energy*. 2011;36:11195-11206.

3. Korkut I, Kasap M, Ciftci I, Seker U. Determination of optimum cutting parameters during machining of AISI 304 steel austenitic stainless steel. *Materials and Design*. 2004;25(4):303-305.

4. Xavior M, Adithan M. Determining the influence of cutting fluids on tool wear and surface roughness during turning of AISI 304 steel austenitic stainless steel. *Journal of Materials Processing Technology*. 2009;209(2):900-909.

5. Cheng CQ, Klinkenbergb LI, Ise Y, Zhao J, Tada E, Nishikata A. Pitting corrosion of sensitised type 304 steel stainless steel under wet–drycycling condition. *Corrosion Science*. 2017;118:217-226.

6. Lu JZ, Qi H, Luo KY, Luo M, Cheng XN. Corrosion behaviour of AISI 304 steel stainless steel subjected to massive laser shock peening impacts with different pulse energies. *Corrosion Science*. 2014;80:53-59.

7. Fattah-Alhosseini A, Vafaeian S. Influence of grain refinement on the electrochemical behavior of AISI 430 ferritic stainless steel in an alkaline solution. *Applied Surface Science*. 2016;360:921-928.

8. Lv JL, Guo WL, Liang TX, Yang M. The effects of ball milling time and surface enriched chromium on microstructures and corrosion resistance of AISI 304 steel stainless steel. *Materials Chemistry and Physics*. 2017;197:79-86.

9. Sun GF, Zhang YK, Zhang MK, Zhou R, Wang K, Liu C, et al. Microstructure and corrosion characteristics of 304 steel stainless steel laser-alloyed with Cr–CrB2. *Applied Surface Science*. 2014; 295:94-107.

10. Aparicio M, Jitanu A, Rodriguez G, Degnah A, Al-Marzoki K, Mosa J, et al. Corrosion protection of AISI 304 steel stainless steel with melting gel coatings. *Electrochimica Acta*. 2016;202:325-332.

11. Mondal J, Marques A, Aarik L, Kozlova J, Simões A, Sammelselg V. Development of a thin ceramic-graphene nanolaminate coating for corrosion protection of stainless steel. *Corrosion Science*. 2016;105:161-169.

12. Krishna N, Thinaharan C, George RP, Parvathavarthini N, Mudali KM. Surface modification of type 304 steel stainless steel with duplex coatings for corrosion resistance in sea water environments. *Surface Engineering*. 2015;31(1):39-47.

13. Almomani M, Hayajneh MT, Al-Daraghmeh MY. The corrosion behavior of AISI 304 stainless steel spin coated with ZrO2-gelatin nanocomposites. *Material Research Express*. 2018; 6:0965c4. Available from: https://doi.org/10.1088/2053-1591/aaeea0

14. Ferreira CC, Ricci VP, Sousa LL, Mariano NA, Campos MGN. Improvement of titanium corrosion resistance by coating with poly-caprolactone and poly-caprolactone/titanium dioxide: potential application in heart valves. *Materials Research*. 2017;20(Suppl 1):126-133.

15. Cui LY, Qin PH, Huang XL, Yin Z|, Zeng R, Li S, et al. Electrodeposition of TiO2 layer-by-layer assembled composite coating and silane treatment on mg alloy for corrosion resistance. *Surface and Coating Technology*. 2017;324:560-568.

16. Yu J, Ji G, Liu Q, Zhang J, Shi Z. Effect of sol-gel ZrO_2 films on corrosion behavior of the 304 steel stainless steel in coal-gases environment at high temperature. *Surface and Coatings Technology*. 2017;331:21-26.

17. Majdia M, Danaeea I, Afghahi S. Preparation and anti-corrosive properties of cerium oxide conversion coatings on steel X52. *Materials Research*. 2017;20(2):445-451.

18. Bu A, Wang J, Zhang J, Bai J, Shi Z, Lu Q, et al. Corrosion behavior of ZrO_2–TiO_2 nanocomposite thin films coating on stainless steel through sol–gel method. *Journal of Sol-Gel Science and Technology*. 2017;81(3):633-638.

19. El-Lateef HMA, Khalaf MM. Corrosion resistance of ZrO_2–TiO_2 nanocomposite multilayer thin films coated on carbon steel in hydrochloric acid solution. *Materials Characterization*. 2015;108:29-41.

20. Cai Y, Quan X, Li G, Gao N. Anticorrosion and scale behaviors of nanostructured ZrO_2–TiO_2 coatings in simulated geothermal water. *Industrial and Engineering Chemistry Research*. 2016;55(44):11480-11494.

21. Olad A, Azhar FF. The synergetic effect of bioactive ceramic and nanoclay on the properties of chitosan–gelatin/nanohydroxyapatite–montmorillonite scaffold for bone tissue engineering. *Ceramics International*. 2014;40(7):10061-10072.

22. Frantiska F, Esther M, Begoña F. Electrophoretic deposition of gelatin/hydroxyapatite composite coatings onto a stainless steel substrate. *Key Engineering Materials*. 2015;654:195-199.

23. Torkaman R, Darvishi S, Jokar M, Kharaziha M, Karbasi M. Electrochemical and in vitro bioactivity of nanocomposite gelatin-forsterite coatings on AISI 316 l stainless. *Progress in Organic Coatings*. 2017;103:40-47.

24. Nomani J, Pramanik A, Hilditch TB, Littlefair G. Chip formation mechanism and machinability of wrought duplex stainless steel alloys. *International Journal of Advanced Manufacturing Technology*. 2015;80(5-8):1127-1135.

25. Fallet M, Mahdjoub H, Gautier B, Bauer JP. Electrochemical behavior of ceramic sol-gel coatings on mild steel. *Journal of Non-Crystalline Solids*. 2001;293(1):527-533.